THE JOURNAL OF CHEMICAL PHYSICS VOLUME 59, NUMBER 10 15 NOVEMBER 1973

# Emission spectra of xenon impurity states in solid and liquid krypton

Ori Cheshnovsky, Baruch Raz, and Joshua Jortner
*Department of Chemistry, Tel-Aviv University, Tel-Aviv, Israel*
(Received 17 April 1973)

In this paper we present the results of an experimental study of electronic energy transfer in xenon–krypton liquid and solid alloys. The $\alpha$-induced luminescence of these dense systems consists of three emission bands which are assigned to the host $Kr^*_2$ molecule, the guest XeKr* heteronuclear molecules, and the $Xe_2^*$ homonuclear molecule. Electronic energy transfer occurs via dipole–dipole coupling between $Kr_2^*$ and Xe single impurity states in the liquid and in the solid as well as to impurity aggregates in the solid. The critical radii for energy transfer were evaluated as $R_q = 25$ Å in the solid at 110 °K and estimated to be $R_q \simeq 24$ Å in the liquid at 120 °K, while the second order perturbation theory results in the values $R_q = 15$ Å for the solid and $R_q = 21$ Å for the liquid. A dramatic decrease of the efficiency and energy transfer with decreasing temperature was observed, which is consistent with the proposed energy transfer mechanism. Some information regarding diffusion controlled reactions in liquid rare gases is reported.

## I. INTRODUCTION

Efficient exciton trapping processes in pure solid and liquid Ar, Kr, and Xe result in the formation of homonuclear rare gas diatomic molecules[1–3] whose emission spectra are practically identical with the second continuum of rare gases excited at moderate ($p > 100$ torr) pressures in the gas phase.[4] Spectroscopic studies of the emission spectra of solid and liquid rare gas alloys are of interest because of several reasons: (a) the investigation of the emission spectra of deep impurity states in dense rare gases is of interest for the understanding of nonradiative transitions between highly excited Wannier states and the nature of medium relaxation around deep impurity states in filled-shell insulators. (b) These studies may provide information regarding the formation of new heteronuclear diatomic excited rare gas molecules. (c) The formation of excited impurity diatomic molecules and their subsequent radiative decay provides information concerning medium induced intramolecular vibrational relaxation in solid and liquid rare gases. (d) The understanding of electronic energy transfer mechanisms from a host diatomic excited molecule to impurity states is of interst.

The emission spectra of rare gas alloys were studied by Basov *et al.*[3] for solid Xe/Kr, by Belov *et al.*[5] for solid Xe/Ar, Xe/Kr, and Kr/Ar, and by the present authors[6] for solid and liquid Xe/Ar mixtures. The interpretation of the emission data of Basov *et al.*[3] and of Belov *et al.*[5] are fraught with difficulties as ultrapure samples (impurity content less than 1ppm) have to be employed in such studies.[6] We have recently reported[6] the observation of the emission from the lowest excited impurity state of Xe in solid and liquid argon. These studies provided spectroscopic evidence regarding medium relaxation resulting in a cavity formation surrounding the single impurity center, thus elucidating point (a). Concerning point (b), Basov *et al.*,[3] the present authors,[6] and Belov *et al.*[5] have assigned some broad emission bands of solid Xe/Kr[3,5,6] and Kr/Ar[5] to emission from heteronuclear diatomic rare gas molecules. Such an assignment is dangerous in view of the occurrence of multiple trapping sites for single and double impurity centers in solid rare gas alloys,[7] so that these emissions may originate from a homonuclear impurity molecule perturbed by the medium. An unambiguous identification of a heteronuclear rare gas diatomic molecule requires the observation of an analogous emission in the gas phase and in the liquid alloy. Regarding point (c), Gedanken *et al.*[8] have recently studied the emission spectra of homonuclear rare gas impurity molecules in solid rare gases, elucidating the nature of the retardation of the formation of $Ne_2^*$ in solid Ne. Finally, no quantitative information is yet available on the nature of electronic energy transfer in solid or liquid rare gases [point (d)]. The mechanisms of electronic energy transfer in gaseous rare gas mixtures were recently investigated in this laboratory,[9] and the extension of the studies to dense phases will be of interest. In this note we present the results of experimental study of electronic energy transfer in liquid and solid xenon–krypton alloys.

## II. EXPERIMENTAL PROCEDURES

The emission from solid and liquid alloys of rare gases bombarded with $\alpha$ particles was monitored by a 0.3 m crossed Czerny Turner spectrograph (McPherson 218). The light was detected using a converter consisting of a sodium salicylate coated Pyrex plate, mounted in front of a EMI 9514S photomultiplier cooled to 220 °K. Spectral emission data were obtained in the range 1100 to 3000 Å. Slitwidths between 0.5 and 2.0 mm were used resulting in resolution of 6.5–26 Å.

The optical cell[10] was characterized by a 1 cm path length. The 0.5 mC Americium $\alpha$ source replaced the back window of the cell, while the front window consisted of a LiF disk 2 mm thick. The cell was mounted on a variable temperature cryostat (Ricor Ein-Harod). The temperature could be varied in the range 80-300 °K and controlled within ± 0.5 °K. The temperature region 80-40 °K was studied by attaching the cell to a cryotip (Air Products).

Matheson research grade rare gases were used. The major impurity content of the Kr gas consisted of 11 ppm Xe, 2 ppm $N_2$ and 1 ppm $O_2$. Rare gas Xe/Kr mixtures (Xe impurity doping level 5-25 000 ppm) were prepared in a bakeable metal vacuum system connected to the optical cell, where an initial pressure of $10^{-7}$ torr was achieved prior to the introduction of the gas mixtures. The gaseous mixtures were then liquified in the cell at a pressure of 1000 torr. Doped solid rare gases were prepared by a moderately slow cooling (0.5 °K/min) of the liquid under pressure of 1000 torr. This procedure resulted in optically transparent 1 cm thick solid Kr doped with Xe, which was perfectly suitable for emission studies. The Xe impurity content in the liquid and solid samples prepared by these procedures was assumed to be equal to that of the composition of the gaseous sample. Optical absorption studies of Xe/Kr 1 cm thick liquid and solid matrices (Xe doping level 1-10 ppm) indicates that the Xe enrichment factor of the samples prepared by this method is negligibly small.

## III. EXPERIMENTAL RESULTS AND DISCUSSION

### A. Spectroscopic Assignments

The emission spectra of solid krypton doped with xenon [Xe/Kr(s)] and of liquid krypton doped with xenon [Xe/Kr(l)] displayed in Figs. 1 and 2 exhibit the following emission bands: (a) A broad emission band peaking at 1480 Å dominates the spectra of solid and liquid krypton alloys at low (< 100 ppm) xenon concentrations, and decreases with increasing xenon concentrations (see Fig. 3). This peak, which is also exhibited by the gaseous liquid and solid Kr, is assigned to the host $Kr_2^*$ $^{1,3}\Sigma_u \to {}^1\Sigma_g$ emission.[11] (b) Liquid Xe-Kr alloys at $[Xe] \gtrsim 50$ ppm exhibit a broad emission band at 1720 Å, which coincides with the emission of pure gaseous Xe (at $p > 100$ torr) and of liquid Xe.[1] This band is assigned to the $Xe_2^*$ impurity $^{1,3}\Sigma_u \to {}^1\Sigma_g$ emission. The formation of $Xe_2^*$ requires molecular diffusion and it is thus not surprising that this 1720 Å band is absent in the Xe/Kr(s) alloy up to $[Xe] \approx 2000$ ppm. For higher (> 2000 ppm) Xe concentrations, the 1720 Å emission is exhibited in the solid alloy due to electronic energy transfer to impurity pairs, resulting in $Xe_2^*$ formation in the solid. (c) A band peaked at 1580 Å appears both in Xe/Kr(s) and Xe/Kr(l). In the liquid mixture this band already appears at low Xe concentrations (> 10 ppm), and its relative intensity reaches a maximum at ~ 100 ppm Xe and starts decreasing (in favor of the $Xe_2^*$ 1720 Å band) at higher Xe concentrations (see Fig. 3). This emission band is assigned to the heteronuclear diatomic KrXe* molecule on the basis of the following arguments: (1) This band appears at relatively low Xe concentrations and thus contains one Xe atom. (2) This band appears both in the liquid and in the solid. (3) An analogous molecular band peaking at 1530 Å was observed in the Xe/Kr gaseous mixtures.[9]

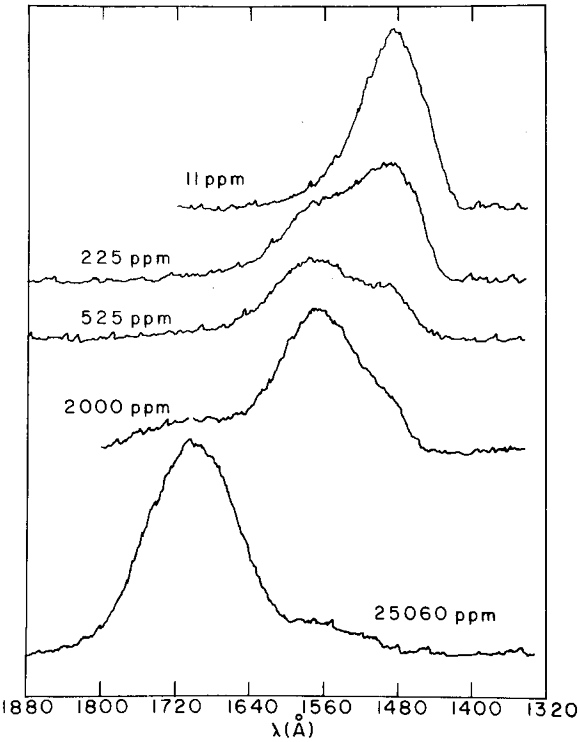

FIG. 1. Emission spectra of solid krypton doped with xenon at various concentrations ($T = 110$ °K).

Several alternative interpretations were considered and rejected: (1) We do not assign this band to the first continuum of vibrationally unrelaxed $Xe_2^*$ because of two reasons. First, this band is observed in the solid at low Xe concentration where impurity aggregation effects are negligible. Second, we expect that vibrational relaxation of the $Xe_2^*$ molecule, which is characterized by a low vibrational frequency (140 cm$^{-1}$),[14] will be efficient in dense phases, whereupon emission will not occur from the vibrationally hot molecule. (2) We do not assign this emission to originate from a trapping site in the solid where the medium perturbations exert a large blue shift on the $Xe_2^*$ "normal" 1720 Å emission,[3,15] as an analogous emis-

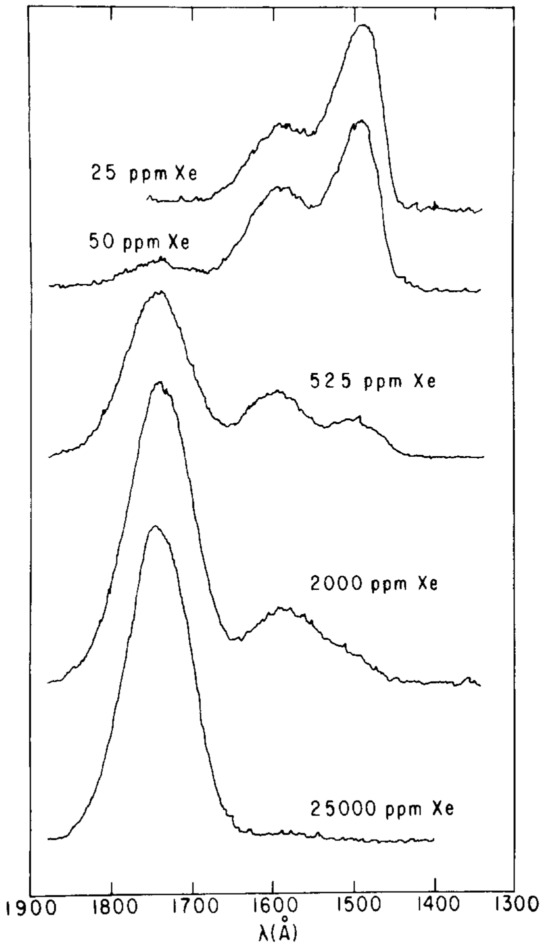

FIG. 2. Emission spectra of liquid krypton doped with xenon at various concentrations ($T = 120$ °K).

sion band is observed in the liquid. (3) We are reluctant to assign this emission to an ionic excited molecule KrXe$^+$ as electron–ion recombination processes are expected to be very efficient in view of the high (~2000 cm$^2$ volt$^{-1}$ · sec$^{-1}$) electron mobility in these systems,[16] and as no evidence was obtained for ionic mechanisms in the formation of the homonuclear diatomic excited rare gases.

### B. Energy Transfer Routes

The energy transfer and energy conversion processes in dense Xe/Kr matrices which result in the impurity molecular emissions can be described as follows: (1) Energy transfer from Kr$_2^*$ ($^1\Sigma_u$ or $^3\Sigma_u$) to the Xe impurity states via a long range energy transfer mechanism. This molecule–impurity atom energy transfer is induced by long range dipole–dipole coupling, the transition probability being determined by the transition moments of the donor and of the acceptor and by the spectral overlap between the donor emission and the acceptor absorption spectra.[9] Both for Xe/Kr(s) and for Xe/Kr(l) (see Fig. 4) spectral overlap determines the energy transfer route from Kr$_2^*$ to the dipole allowed Xe $n = 1$ ($^2P_{3/2}$) state. (2) The impurity Xe $n = 1$ ($^2P_{3/2}$) state which corresponds to the $^3P_1$ atomic configuration can be quenched nonradiatively to the metastable Xe ($^3P_2$) state, which is dipole forbidden to the ground state. (3) The heteronuclear XeKr* excited molecule can be formed from Xe($^3P_1$) + Kr($^1S_0$) or from Xe($^3P_2$) + Kr($^1S_0$).

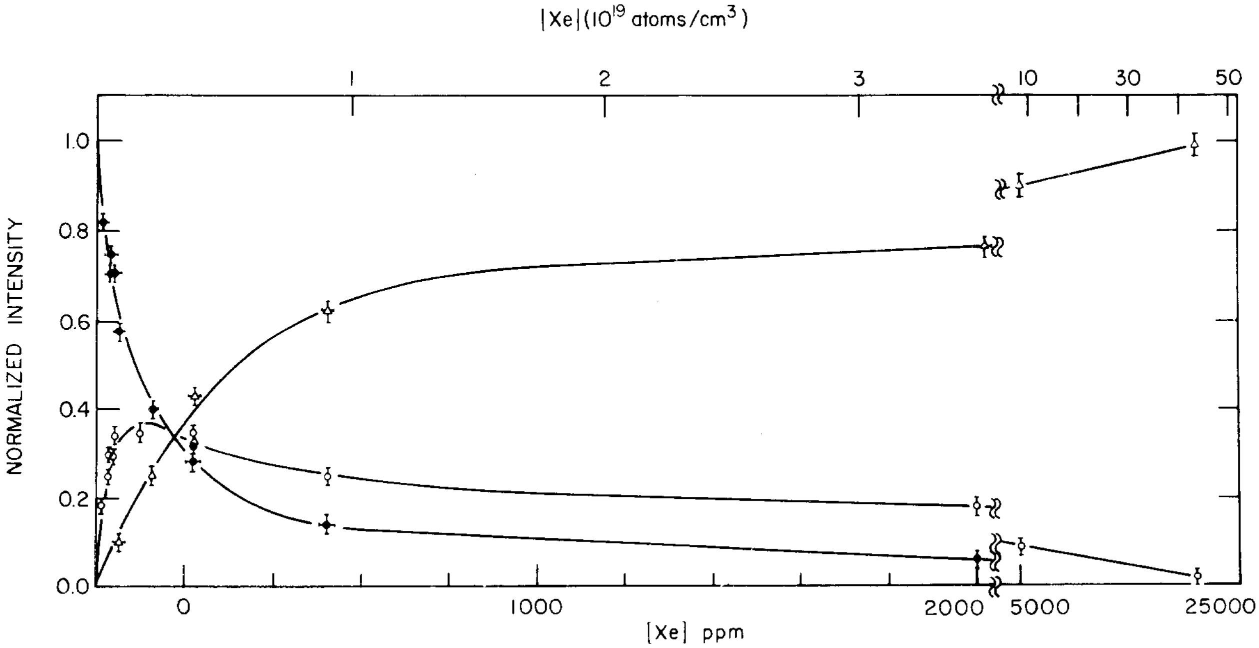

FIG. 3. Normalized emissions from xenon impurities vs xenon concentration in xenon-doped liquid krypton at 120 °K.

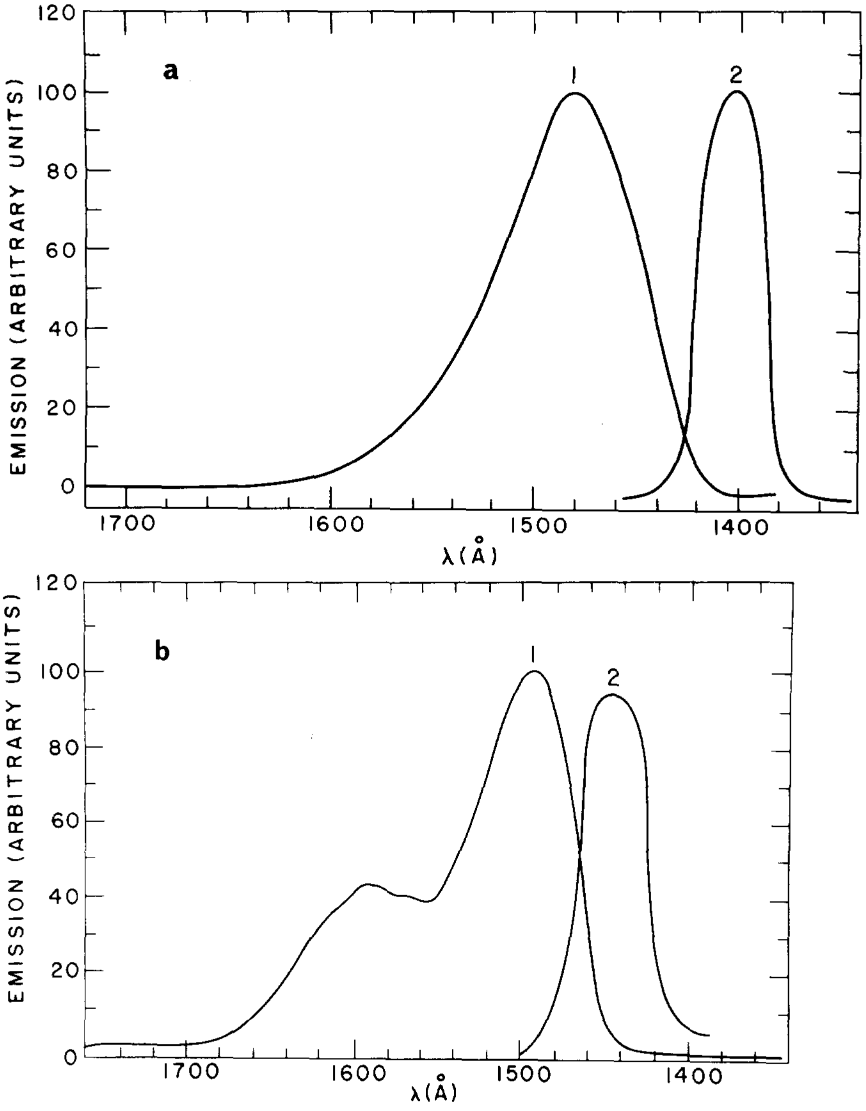

FIG. 4. Superposition of the krypton matrix emission spectra 1 and the xenon impurity absorption spectra 2 in solid krypton (a), and in liquid krypton (b).

(4) In liquid krypton, xenon diffusion results in the interconversion of the heteronuclear molecule to the homonuclear impurity molecule $XeKr^* + Xe(^1S_0) \rightarrow Xe_2^*(^{1,3}\Sigma_u) + Kr(^1S_0)$. (5) At high Xe concentration in the solid Kr electronic energy transfer from $Kr_2^*$ to Xe aggregates (whose absorption spectrum is only slightly ~ 500 $cm^{-1}$ red shifted relative to the single impurity Xe absorption)[17] leads to the formation of $Xe_2^*(^{1,3}\Sigma_u)$.

The efficiency of molecule–atomic impurity electronic energy transfer process is determined in terms of the critical transfer radius $R_q$,[18] where the probability of the radiative decay of the $Kr_2^*$ acceptor is equal to the energy transfer probability. Second order perturbation theory results in the following expression[18]:

$$R_q = (\lambda_3 \mu_A^2 F / 8\pi^2)^{1/6}, \qquad (1)$$

where λ is the (mean) wavelength for the donor emission, $\mu_A$ is the transition moment for the acceptor absorption, while $F$ corresponds to the spectral overlap function

$$F = \int_0^\infty f_{Aa}(E) f_{De}(E)\, dE, \qquad (2)$$

where $f_{Aa}(E)$ and $f_{De}(E)$ represent the normalized acceptor (Xe) absorption and the donor ($Kr_2^*$) emission line shapes, respectively. The transfer radius is essentially determined by the spectral overlap function.

We can now perform a theoretical estimate of $R_q$, utilizing our $Kr_2^*$ emission spectra and the detailed absorption spectra of Ophir[19] for the $n = 1$ $(^3P_{3/2})$ state of Xe/Kr in thick crystals. We express the two line shapes in terms of Gaussian functions

$$f_{Aa}(E) = (\pi\xi^2)^{-1/2} \exp(-E^2/\xi^2) \qquad (3a)$$

and

$$f_{De}(E) = (\pi\Delta^2)^{-1/2}\exp[-(E_a - E)^2/\Delta^2], \qquad (3b)$$

where $\Delta$ and $\xi$ are the second moments of the emission and absorption bands, while $E_A$ represents the energy of the maximum of the Xe impurity absorption relative to the maximum of Kr$_2^*$ emission. The spectral overlap function [Eq. (2)] is

$$F = [\pi(\Delta^2 + \xi^2)]^{-1/2}\exp[-E_A^2/(\Delta^2 + \xi^2)]. \qquad (4)$$

To estimate $R_q$ at 110 °K we take $\Delta = 2160$ cm$^{-1}$ and from Ophir's results[19] $E_A = 3950$ cm$^{-1}$ and $\xi = 690$ cm$^{-1}$. Equations (1)–(4) then yield $F = 1.2 \times 10^{-5}$ cm and $R_q = 15$ Å for Xe/Kr(s) at 110 °K. It is interesting to note that $R_q$ and subsequently the electronic transfer probability in this system should exhibit a sharp temperature dependence in view of the following features: (a) The position of the absorption band of the Xe impurity exhibits a marked temperature dependence, shifting to higher energies with decreasing temperature. From Ophir's data[19] we get that $E_A$ changes from 3950 cm$^{-1}$ at 110 °K to 4870 cm$^{-1}$ at 40 °K. (b) The width of the Xe absorption band exhibits a marked temperature dependence due to conventional phonon broadening,[19] changing from $\xi = 690$ cm$^{-1}$ at 110 °K to $\xi = 440$ cm$^{-1}$ at 40 °K. (c) $\Delta$ is expected to exhibit a temperature dependence of the form $\Delta = \Delta_0[\coth(\hbar\omega/2kT)]^{1/2}$,[14,20] where $\Delta_0 = 2940$ cm$^{-1}$ at low temperatures[7] and $\hbar\omega$ is the molecular vibrational frequency. From Mulliken's estimates[21] we take $\hbar\omega = 190$ cm$^{-1}$ for Kr$_2^*$, which lies between the experimental values[14] $\hbar\omega = 140$ cm$^{-1}$ for Xe$_2^*$ and $\hbar\omega = 310$ cm$^{-1}$ for Ar$_2^*$. Making use of these data and Eq. (4) we get that the spectral overlap is reduced from $F = 1.2 \times 10^{-5}$ cm at 110 °K to $F = 0.90 \times 10^{-6}$ cm at 40 °K, whereupon $R_q$ changes from 15 to 9.7 Å in this temperature range. As the energy transfer probability is determined by $R_q^{+3}$, i.e., $F^{1/2}$, we expect that the efficiency of electronic energy transfer in solid Xe/Kr is reduced by a factor of 3.7 in the temperature range 110–40 °K.

Finally we would like to provide an estimate for $R_q$ in liquid Xe/Kr alloys. Utilizing the available absorption data[13] we now have at 120 °K $\Delta = 1550$ cm$^{-1}$, $\xi = 1890$ cm$^{-1}$, $E_A = 2170$ cm$^{-1}$, and Eq. (4) gives us $F = 1.05 \times 10^{-4}$ cm and $R_q = 21$ Å for the liquid.

### C. Electronic Energy Transfer in Solid Xe/Kr

Utilizing the Förster[18] theory for the electronic energy transfer in the solid alloy, the quantum yield $A$ for the acceptor emission at the acceptor concentration $C$ is given by

$$A = (\eta^0 - \eta)/\eta^0 = \sqrt{\pi}\, q \exp(q^2)[1 - \mathrm{erf}(q)], \qquad (5)$$

where $\eta$ is the donor quantum yield and $\eta = \eta^0$ at $C = 0$ and

$$q = \tfrac{1}{2}\sqrt{\pi}\, C/C_0, \qquad (6)$$

with $C_0$ being the critical concentration

$$C_0 = 3/4\pi R_q^3. \qquad (7)$$

From the experimental data for the solid xenon-krypton alloy we have calculated the intensity ratio $I(\mathrm{Kr}_2)/\sum I(\mathrm{Xe})$, where $I(\mathrm{Kr}_2)$ is the intensity of the donor (i.e., 1480 Å band) while $\sum I(\mathrm{Xe})$ corresponds to the total acceptor emission intensity (i.e., the sum of the 1580 and the 1720 Å bands). The intensity ratio $I(\mathrm{Kr}_2)/I(\mathrm{Xe})$ equals $(A^{-1} - 1)$, where $A$ is given by Eq. (5). The dependence of this intensity ratio on the Xe concentration (Fig. 5) fits well Eqs. (5)–(7), resulting in $R_q = 25$ Å for Xe/Kr(s) at 100 °K. This value is in fair agreement with the theoretical estimate $R_q = 15$ Å (see Sec. III.B).

A further support for the applicability of the dipole–dipole resonance energy transfer mechanism to this system is obtained from the temperature dependence of the energy transfer probability in Xe/Kr(s). As is evident from Fig. 6, the acceptor emission, at constant Xe concentration, observed at 1580 Å decreases with decreasing temperature. This effect is attributed to the narrowing of and the blue shift of $f_{aA}(E)$[19] of the impurity absorption and to the simultaneous narrowing of $f_{ED}(E)$ of the emission of the Kr$_2^*$ with decreasing temperature.

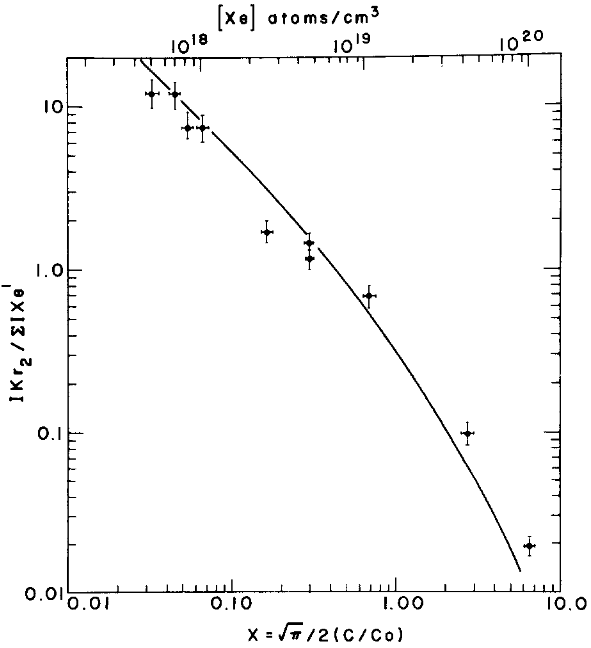

FIG. 5. Dependence of the ratio of krypton donor emission to xenon acceptor emission upon the acceptor concentration (● represents experimental points). The solid line is a fit of Förster's theoretical curve [Eqs. (5)–(7)].

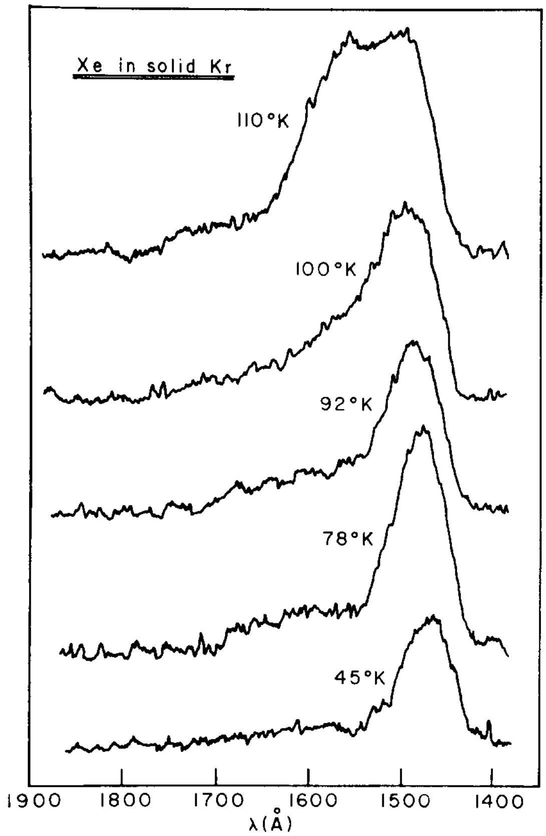

FIG. 6. Emission spectra of xenon-doped solid krypton at different temperatures. Xe concentration 500 ppm.

The experimental data of Fig. 6 exhibit a change of ($A^{-1}-1$) from 1.15 at 110 °K to 4.25 at 65 °K, whereupon $C_0$ decreases by a numerical factor of 3.2 in the temperature region 110–65 °K. This result (Fig. 7) is in good agreement with the calculations based on Eqs. (1)–(4), using Ophir's absorption data, as described in the previous section.

In the analysis of the electronic energy transfer process in the solid we have conscientiously disregarded the contribution of energy, i.e., exciton migration in the solid. If such energy migration processes were of importance they may affect the details of the semiquantitative analysis of the experimental data.[22] The absence of the emission from the $n=1$ ($^2p_{3/2}$) exciton state, which results from efficient exciton trapping process in pure condensed rare gases, provides conclusive experimental evidence that the lifetime of a "free" exciton in solid (and liquid rare gases) is shorter than $10^{-11}$ sec. Thus in the Ke/Kr condensed systems where reasonably good spectral overlap between $Kr_2^*$ ($^{1,3}\Sigma_u \rightarrow {}^1\Sigma_g$) and Xe ($^1S_0 \rightarrow {}^3P_1$) for electronic energy transfer involves the $Kr_2^*$/Xe transfer. The trapped exciton, which consists of the diatomic molecule, is characterized by a relatively high binding energy[21] of ~0.5 eV. We thus expect that the diffusion of the trapped exciton in the solid is exceedingly low,[23] as may be argued on the basis of the low hole mobility data in solid rare gases, where the positive hole consists of a diatomic molecular ion. Thus the only relevant energy migration processes in this host matrix involves diffusive mass transfer in the liquid.

### D. Electronic Energy Transfer in Liquid Xe/Kr

The electronic energy transfer and energy conversion processes in the liquid mixture can be represented in terms of the kinetic scheme

$$\mathrm{Kr}_2^*(^3\Sigma_u) \xrightarrow{\tau_1^{-1}} 2\,\mathrm{Kr}(^1S_0) + h\nu_1, \tag{8a}$$

$$\mathrm{Kr}_2^*(^3\Sigma_u) + \mathrm{Xe}(^1S_0) \xrightarrow{k_P} \mathrm{Xe}^*(^3P_1), \tag{8b}$$

$$\mathrm{Xe}^*(^3P_1) \xrightarrow{k_C} \mathrm{Xe}^*(^3P_2), \tag{8c}$$

$$\mathrm{Xe}^*(^3P_1) \text{ or } \mathrm{Xe}^*(^3P_2) \xrightarrow{k_E} \mathrm{XeKr}^*, \tag{8d}$$

$$\mathrm{XeKr}^* \xrightarrow{\tau_2^{-1}} \mathrm{Xe}(^1S_0) + \mathrm{Kr}(^1S_0) + h\nu_2, \tag{8e}$$

$$\mathrm{XeKr}^* + \mathrm{Xe}(^1S_0) \xrightarrow{k_F} \mathrm{Xe}_2^*(^3\Sigma_u)\ , \tag{8f}$$

$$\mathrm{Xe}_2^*(^3\Sigma_u) \xrightarrow{\tau_3^{-1}} 2\,\mathrm{Xe}(^1S_0) + h\nu_3, \tag{8g}$$

where we have assumed that in the dense medium reaction (8c) for the deactivation of $Xe^*(^3P_1)$ and the analogous process for the activation of $Kr^*(^3P_1)$ is efficient. Thus the lifetimes of the three diatomic molecules will be taken to be equal to that of the $^3\Sigma_u$ state of $Kr_2^*$.[9]

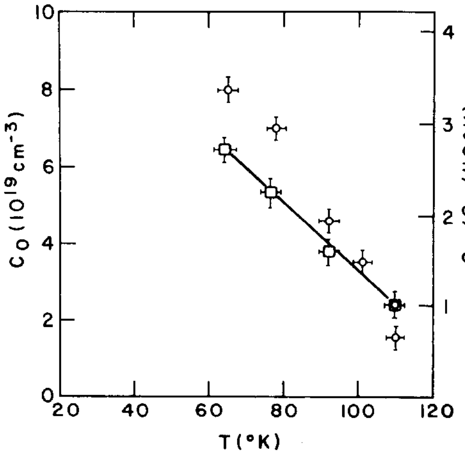

FIG. 7. Temperature dependence of Förster's critical concentration $C_0$. □ represents $C_0$ calculated from Ophir's xenon impurity state absorption spectra[19] and from our pure krypton emission spectrum. ○ represents relative critical concentrations evaluated from the experimental data given in Fig. 6.

Under steady state conditions the normalized emission intensities $I(\mathrm{Kr}_2^*)$, $I(\mathrm{KrXe})$, and $I(\mathrm{Xe}_2)$ normalized to the total intensity $\sum I$, are given by

$$I(\mathrm{Kr}_2^*)\Big/\sum I = 1/(1+a[\mathrm{Xe}]), \qquad (9)$$

$$I(\mathrm{KrXe}^*)\Big/\sum I = a[\mathrm{Xe}]/(1+a[\mathrm{Xe}])(1+b[\mathrm{Xe}]), \qquad (10)$$

$$I(\mathrm{Xe}_2^*)\Big/\sum I = ab[\mathrm{Xe}]/(1+a[\mathrm{Xe}])(1+b[\mathrm{Xe}]), \qquad (11)$$

where

$$a\,k_D\tau_1, \quad b = k_F\tau_2.$$

To analyze the experimental data on Fig. 3, we utilize the relations which are immediately obtained from Eq. (9)–(11).

$$[I(\mathrm{KrXe}^*)+I(\mathrm{Xe}_2^*)]/I(\mathrm{Kr}_2^*) = k_D\tau_1[\mathrm{Xe}], \qquad (12)$$

$$I(\mathrm{Xe}_2^*)/I(\mathrm{KrXe}^*) = k_F\tau_2[\mathrm{Xe}]. \qquad (13)$$

The linear plot of the left-hand side of Eq. (13) vs [Xe] (Fig. 8) provides strong quantitative support for the identification of the $\mathrm{KrXe}^*$ heteronuclear diatomic molecule as an intermediate in the formation of the homonuclear $\mathrm{Xe}_2^*$ molecule. From Fig. 8 we get $b = 5\times10^8$ cm$^{-3}$. Assuming that the major molecular emission of $\mathrm{KrXe}^*$ originates from the state formed from $\mathrm{Xe}(^3P_2)$ metastable we take $\tau_2 = 10^{-6}$ sec (equal to the lifetime of $^3\Sigma_u$ state of $\mathrm{Kr}_2^*$).[9b] Thus we get $k_F = 2\times10^{-13}$ cm$^3$ sec$^{-1}$. This value is consistent with the rate of a diffusion controlled reaction $k_F = 4\pi D^*R$, where $R$ is the encounter radius and $D^*$ is the relative diffusion coefficient. Taking $D^* = 10^{-6}$ cm$^2$ sec$^{-1}$ (which is somewhat lower than the self-diffusion of liquid Ar, $D \approx 10^{-5}$ cm$^2$ sec$^{-1}$)[24] and $R = 5$ Å we estimate $k_F = 6\times10^{-13}$ cm$^3$ sec$^{-1}$.

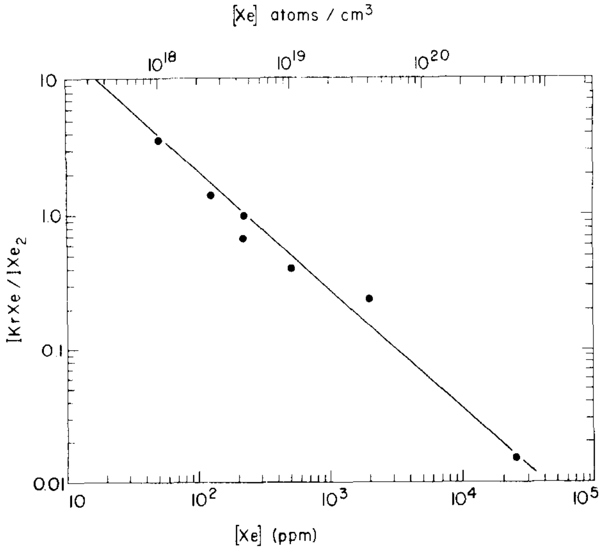

FIG. 8. Dependence of the intensity ratio of the heteronuclear excited $\mathrm{KrXe}^*$ molecule emission to the excited homonuclear diatomic $\mathrm{Xe}_2^*$ molecular emission upon the Xe concentration in liquid krypton.

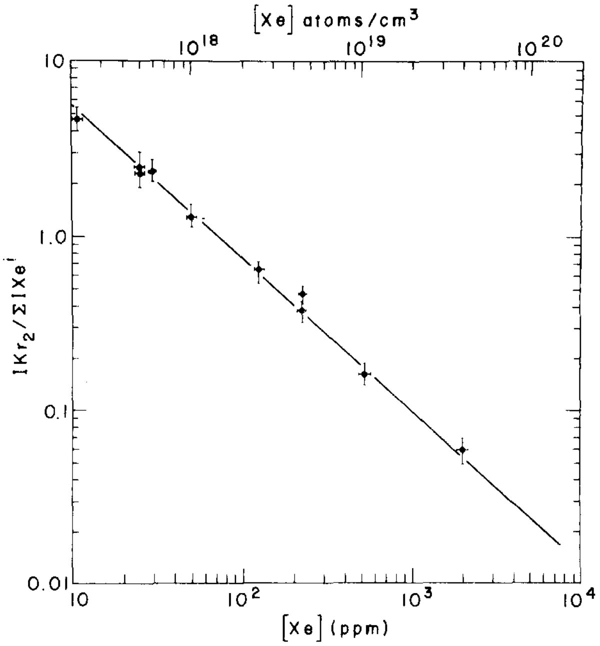

FIG. 9. Dependence of the ratio of the emission from the $\mathrm{Kr}_2^*$ donor molecule to the total emission from the xenon impurity upon the impurity concentration in liquid krypton.

The energy transfer rate constant $k_D$ is evaluated from Eq. (12) and the experimental data of Fig. 3. From the linear plot of the left-hand side of Eq. (12) vs [Xe] (Fig. 9) we get $a = 6.2\times10^{-19}$ cm$^3$. Taking $\tau_1 = 10^{-6}$ sec (i.e., the lifetime of the $^3\Sigma_u$ state) we obtain $k_D = 6.2\times10^{-13}$ cm$^3$ sec$^{-1}$.

The energy transfer rate constant $k_D$ involves long range electronic energy transfer coupled with diffusive motion. The approximate theoretical treatment of Taninoto and Yokota[25] demonstrated that the energy transfer process can be expressed in terms of a bimolecular rate constant provided that

$$D^*R_q^{-2}\,t^{2/3}/\tau^{1/3} \gg 1, \qquad (14)$$

which implies that the distance traversed by the excited molecule during its lifetime considerably exceeds $R_q$. For $\tau_1 \sim 10^{-6}$ sec, this condition is satisfied for $t > 10^{-9}$ sec. In this case, the rate constant for electronic energy transfer is

$$k_D = (0.51)4\pi(R_q^6\tau_1^{-1})^{1/4}D^{*\,3/4}. \qquad (15)$$

Making use of the kinetic value for $k_D$ obtained from Fig. 9 we can estimate $R_q$ in the liquid for Eq. (15). Taking $D^* \sim 10^{-6}$ cm$^2$ sec$^{-1}$, which is consistent with the assumption that $k_F$ is a diffusion-controlled reaction, and $\tau_1 = 10^{-6}$ we estimate $R_q \simeq 24$ Å as an approximate value for the transfer radius in the liquid. The value of $R_q = 24$ Å for the liquid is close to the calculated value (Sec. III B) of 21 Å; however, this good agreement is somewhat fortuitous, as the same theory underestimates $R_q$ in the solid. On the basis of the spectral overlap which is larger in the liquid than in the solid, we expect that for Xe/Kr alloys $R_q(\mathrm{l}) = 1.42R_q(\mathrm{s})$; however, in view of the uncertainty in the diffusion coefficient such a detailed comparison cannot yet be performed.

These results provide a nice example for the applicability of diffusion controlled kinetics to "chemical" reactions (involving excited molecules) in a simple dense fluid.

[1] J. Jortner, L. Meyer, S. A. Rice, and E. G. Wilson, J. Chem. Phys. **42**, 4250 (1965).

[2] O. Cheshnovsky, B. Raz, and J. Jortner, Proceedings of the Third International Vacuum Ultraviolet Spectroscopy Conference, Tokyo, 1971 (unpublished).

[3] N. G. Basov, E. M. Balashov, O. V. Bogdankevitch, V. A. Danilychev, G. N. Kashnikov, N. P. Lantshov, and D. P. Khodkevitch, J. Lumin. **1**, 834 (1970); J. Lumin. **2**, 834 (1970).

[4] The following review articles and references mentioned there: (a) R. E. Huffman, J. C. Larrabee, and Y. Tanaka, Appl. Opt. **4**, 1581 (1965); (b)P. G. Wilkinson and E. T. Byram, Appl. Opt. **4**, 581 (1965).

[5] A. G. Belov, I. Ya. Fugol, and V. Savchenko, Solid State Commun. **12**, 1 (1973).

[6] O. Cheshnovsky, B. Raz, and J. Jortner, J. Chem. Phys. **57**, 4682 (1972).

[7] A. Gedanken, B. Raz, and J. Jortner, "Emission Spectra of Solid Rare Gas Alloys" (unpublished).

[8] A. Gedanken, B. Raz and J. Jortner, "Emission Spectra of Rare Gas Impurity Molecules in Solid Neon" (unpublished).

[9] (a) A. Gedanken, J. Jortner, B. Raz, and A. Szöke, J. Chem. Phys. **57**, 3456 (1972). (b) O. Cheshnovsky, B. Raz, and J. Jortner, "Electronic Energy Transfer in Rare Gas Mixtures" (unpublished).

[10] B. Raz, J. Magen, and J. Jortner, Vacuum **19**, 571 (1969).

[11] The Xe $n = 1(^2P_{3/2})$ impurity state in Kr(s) and in Kr(l) is observed in absorption at 1400 Å[12,13] and at 1445 Å,[13] respectively, while the emission in both dense phases is expected to occur around 1470 Å in view of medium relaxation. Our low spectral resolution does not allow us to separate this band from the $\mathrm{Kr}_2^*$ emission.

[12] G. Baldini, Phys. Rev. **137**, A508 (1965).

[13] B. Raz and J. Jortner, Chem. Phys. Lett. **4**, 511 (1970); Proc. R. Soc. Lond. A 317, 113 (1970).

[14] O. Cheshnovsky, B. Raz, and J. Jortner, Chem. Phys. Lett. **15**, 475 (1972).

[15] A. Gedanken, O. Chesnovsky, B. Raz and J. Jortner, "Temperature Dependence of the Emission of Solid Xenon" (unpublished).

[16] (a) H. Schnyders, S. A. Rice, and L. Meyer, Phys. Rev. **150**, 127 (1966). (b) L. S. Miller, S. Howe, and W. E. Spear, Phys. Rev. **166**, 871 (1968).

[17] G. Baldini, Phys. Rev. **128**, 1562 (1962).

[18] Th. Förster, Ann. Phys. (Leipz.) **2**, 55 (1948).

[19] Z. Ophir, M.Sc. thesis, Tel-Aviv University, Tel-Aviv, Israel, 1970.

[20] J. B. Birks, *Photophysics of Aromatic Molecules* (Wiley, New York, 1970).

[21] R. S. Mulliken, J. Chem. Phys. **52**, 5170 (1970).

[22] For a recent discussion see M. J. Weber, Phys. Rev. B **4**, 2932 (1971).

[23] L. S. Miller, S. Howe, and W. E. Spear, Phys. Rev. **158**, 305 (1967).

[24] J. Naghizadeh and S. A. Rice, J. Chem. Phys. **36**, 2710 (1962).

[25] M. Yokota and O. Tanimoto, J. Phys. Soc. Jap. **22**, 779 (1967).